

ANALYSIS OF VOLUMETRIC PROPERTIES OF LIQUID MIXTURES II. AQUEOUS-ORGANIC SOLVENT SYSTEMS

P. V. Efimov^a, N. V. Efimova^b

V. N. Karazin Kharkiv National University, Education and Research Institute of Chemistry,
4 Svobody sqr., Kharkiv, Ukraine

a) ✉ pavel.v.efimov@karazin.ua

 <https://orcid.org/0000-0003-1781-3844>

b) ✉ n.v.efimova@karazin.ua

 <https://orcid.org/0000-0002-1089-2976>

An extended model of binary additive quasi-solvates (BAQS) is proposed to describe the properties of binary liquid systems. The model incorporates two additional parameters: the limiting partial molar quantities of the solution components. Notably, these parameters are determined a priori, typically from independent experimental data. Concurrently, within the model framework, the effective limiting partial molar quantities are derived from the dependence of the studied property on the mixture composition. The discrepancy between the a priori and effective values is attributed to a shift in the equilibrium between homogeneous and heterogeneous quasi-solvates, as well as a redistribution of the solvent-solute roles within heterogeneous quasi-solvates. For each component, a parameter ξ is introduced, representing the ratio of the effective excess limiting partial molar quantity to its corresponding a priori value. Based on these parameters, the excess functions of heterogeneity α^E and role asymmetry β^E are defined.

Using molar volume dependencies for 12 binary aqueous systems (with methanol, ethanol, 1-propanol, 2-propanol, ethylene glycol, tetrahydrofuran, 1,4-dioxane, acetonitrile, acetone, dimethylformamide, dimethylacetamide, and dimethyl sulfoxide) at 298.15 K, along with literature data, the functions α^E and β^E were calculated. The study determined the compositions and function values at extrema, average function values, and quasi-solvate weighting factors for equimolar mixtures. The results demonstrate that the calculated parameters can effectively characterize structural features of aqueous-organic solutions. Despite the model's apparent simplicity, this approach is suitable for the rapid analysis of large sets of binary liquid systems.

Keywords: physicochemical analysis, molar volume, limiting partial molar volume, aqueous-organic solvent, binary additive quasi-solvates.

Introduction

The structure of aqueous-organic solutions is of significant interest for both theoretical and applied chemistry. This topic has been the subject of numerous experimental and theoretical studies, including molecular modeling [1–11]. However, a vast amount of experimental data accumulated over decades of research remains largely underutilized. Therefore, there is a clear need for a simple, even if qualitative, method to analyze the structural features of mixed liquid systems.

In a previous report [12], the binary additive quasi-solvate (BAQS) model was introduced. The present work develops this model for cases where the "true" values of limiting partial molar volumes are known. It is assumed that these values are obtained from independent experiments. Unfortunately, such data are significantly less common than the mixed liquid systems studied to date (ddbst.com). Nevertheless, when supplementary information about the system is available alongside composition-dependent volumetric properties, it can be effectively utilized in the analysis.

Summary of the Main Provisions of the BAQS Model

1. A mixture of liquids is represented as a collection of quasi-solvates.
2. A quasi-solvate is understood as a pair of particles, where one of them acts as a solvent and the other as a solute. For example, for a mixture of two liquids A and B, there are 4 types of quasi-solvates: Q_{AA} : solvent A, solute A; Q_{BA} : solvent A, solute B; Q_{AB} : solvent B, solute A; Q_{BB} : solvent B, solute B.
3. The totality of each type of quasi-solvate possesses a macroscopic property P_{ij} , where i – is the solute and j – is the solvent, and

$$P_{ij} \neq P_{ji} \quad (1)$$

4. It is assumed that for quasi-solvates formed by identical particles, the property P_{ii} corresponds to the property of the pure liquid. For systems with different particles:

$$P_{ij} = \frac{\bar{P}_{ij}^{\circ} + P_{jj}}{2} \quad (2)$$

where \bar{P}_{ij}° are the limiting partial quantities of the i -th substance in the j -th solvent. Limiting quantities are used because no interaction between quasi-solvates is assumed. Thus, the values of property P are defined as:

$$P = \sum_{i=1}^n \sum_{j=1}^n P_{ij} w_{ij} \quad (3)$$

where w_{ij} are weighting factors.

If a random distribution of the quasi-solvate composition is assumed, the general expression necessarily follows:

$$P = \sum_{i=1}^n \sum_{j=1}^n (\bar{P}_{ij}^{\circ} + P_{jj}) \frac{x_i x_j^2}{x_i + x_j} \quad (4)$$

For binary systems:

$$P = P_{11} x_1^2 + P_{22} x_2^2 + (\bar{P}_{12}^{\circ} + P_{22}) x_1 x_2^2 + (\bar{P}_{21}^{\circ} + P_{11}) x_2 x_1^2 \quad (5)$$

The excess property is defined as:

$$P^E = P - \sum_{i=1}^n P_{ii} x_i \quad (6)$$

For a binary system, taking into account Eq. 5:

$$P^E = x_1 x_2 (\bar{P}_{12}^{E\circ} x_2 + \bar{P}_{21}^{E\circ} x_1) \quad (7)$$

Where $\bar{P}_{ij}^{E\circ}$ is the excess limiting partial molar property for the corresponding pair of solvents. As can be seen, Eq. 7 is a three-suffix Margules equation.

Methodology

Assuming a stochastic distribution of quasi-solvates, the parameters $\bar{P}_{12}^{E\circ}$ and $\bar{P}_{21}^{E\circ}$ will be the effective excess limiting partial quantities. They can be determined from a data set by linear approximation of Eq. 7. However, the distribution of quasi-solvates may be non-stochastic. Therefore, it is necessary to take into account the following deviations from equilibrium for heterogeneity and role asymmetry, respectively:

$$Q_{11} + Q_{22} \rightarrow Q_{12} + Q_{21} \quad (8)$$

$$Q_{21} \rightarrow Q_{12} \quad (9)$$

Then the weighting factors will be expressed as:

$$w_{11} = x_1^2 - \alpha^E \quad (10)$$

$$w_{22} = x_2^2 - \alpha^E \quad (11)$$

$$w_{12} = 2 x_1 x_2^2 + \alpha^E + \beta^E \quad (12)$$

$$w_{21} = 2 x_2 x_1^2 + \alpha^E - \beta^E \quad (13)$$

Where α^E and β^E are the mole fractions corresponding to deviations from the base model. The determination of this deviation and its associated quantities constitutes the task of the proposed analysis. Taking into account Eqs. 10-13, the excess property will be defined as:

$$P^E = x_1 x_2 (\bar{P}_{12}^{E\infty} x_2 + \bar{P}_{21}^{E\infty} x_1) + \frac{1}{2} \alpha^E (\bar{P}_{12}^{E\infty} + \bar{P}_{21}^{E\infty}) + \frac{1}{2} \beta^E (\bar{P}_{12}^{E\infty} - \bar{P}_{21}^{E\infty}) \quad (14)$$

Where $\bar{P}_{ij}^{E\infty}$ are the "true" excess limiting partial quantities.

Equating P^E from Eq. 7 and Eq. 14, we obtain:

$$x_1 x_2 ((\bar{P}_{12}^{E\circ} - \bar{P}_{12}^{E\infty}) x_2 + (\bar{P}_{21}^{E\circ} - \bar{P}_{21}^{E\infty}) x_1) = \frac{1}{2} \alpha^E (\bar{P}_{12}^{E\infty} + \bar{P}_{21}^{E\infty}) + \frac{1}{2} \beta^E (\bar{P}_{12}^{E\infty} - \bar{P}_{21}^{E\infty}) \quad (15)$$

Since the properties of quasi-solvates are additive, Eq. 15 can be decomposed into its components:

$$\left(\bar{P}_{12}^{E^\circ} - \bar{P}_{12}^{E^\infty}\right) x_1 x_2^2 = \bar{P}_{12}^{E^\infty} \left(\frac{1}{2} \alpha^E + \frac{1}{2} \beta^E\right) \quad (16)$$

$$\left(\bar{P}_{21}^{E^\circ} - \bar{P}_{21}^{E^\infty}\right) x_2 x_1^2 = \bar{P}_{21}^{E^\infty} \left(\frac{1}{2} \alpha^E - \frac{1}{2} \beta^E\right) \quad (17)$$

Thus, we obtain a system of equations with two unknowns, α^E and β^E .

Let us introduce the notation:

$$\zeta_i = \frac{\bar{P}_{ij}^{E^\circ}}{\bar{P}_{ij}^{E^\infty}} - 1 \quad (18)$$

Then:

$$\alpha^E = x_1 x_2 (\zeta_1 x_2 + \zeta_2 x_1) \quad (19)$$

$$\beta^E = x_1 x_2 (\zeta_1 x_2 - \zeta_2 x_1) \quad (20)$$

Further analysis will be conducted using Eqs. 19 and 20.

Volumetric analysis of aqueous-organic solvent mixtures

Volumetric properties of aqueous-organic mixtures were chosen as the object of analysis. The choice of systems is due to two factors: wide prevalence and the availability of data on limiting partial volumes from independent experiments. Aqueous mixtures with methanol, ethanol, propanol, isopropanol, ethylene glycol, tetrahydrofuran, 1,4-dioxane, acetonitrile, acetone, dimethylformamide, dimethylacetamide, and dimethyl sulfoxide at 298.15 K and atmospheric pressure were considered. Data on the limiting partial molar volumes of water and organic solvents were taken from literature sources [10, 11, 14, 17, 21, 24, 30, 32-37]. Effective limiting molar partial volumes were calculated by the least squares method from literature data on the dependence of density on the composition of aqueous-organic systems [2, 13, 16].

For all systems, the analysis was performed according to a single scheme. First, the name of the co-solvent is given. A figure of the dependence of the excess molar volume on the mole fraction of the organic component is provided. The dots represent experimental data. The black line shows the approximation by Eq. 7. The green line shows the theoretical calculation curve according to Eq. 7 using independent data for the limiting partial molar volume. The next figure shows the linear approximation of Eq. 21, which can be used to judge the applicability of the BAQS model to the given system

$$\Delta V_N = \frac{V^E}{x_1 x_2} = \bar{V}_{12}^{E^\circ} x_2 + \bar{V}_{21}^{E^\circ} x_1 \quad (21)$$

The third figure shows the dependencies of the functions α^E and β^E on the composition of the organic component. The table provides values of molar volumes of water and organic solvent, literature data for limiting partial molar volumes, calculated data for effective limiting partial volumes, excess limiting partial molar volume, effective excess limiting partial volume, and parameters ξ_w and ξ_s . Also included are the positions and values of maxima and minima, the composition with zero function value, and integral means of α^E and β^E . The integrals of α^E and β^E actually show the averaged deviations from the stochastic distribution of quasi-solvates. All listed characteristics are determined by two parameters, ξ_w and ξ_s . The accuracy of determining these parameters depends on the accuracy of determining the excess quantities, as well as on their absolute values. The error in determining the parameters ξ_w and ξ_s can be estimated as approximately ± 0.1 . The values of the functions α^E and β^E represent the structural characteristics of the solutions. The function α^E can be interpreted as an increase in the probability of finding a heterogeneous quasi-solvate compared to the stochastic distribution of the base model. Positive values correspond to a tendency to form heterogeneous water-organic component quasi-solvates. With some reservations, a correlation can be assumed with parameters obtained from the analysis of the radial distribution function. Therefore, for each system, a comparison is made with the results of molecular modeling, solutions of the Kirkwood-Buff equations, or experimental neutron scattering data. The comparison is made at a qualitative level. The function β^E has no analogues and shows how the distribution of solvent-solute roles changes in heterogeneous quasi-solvates. Positive values indicate an enhancement of the role of the organic component as a solvent and, accordingly, an enhancement of the role of water as a solute compared to the base model.

1. Water-Methanol

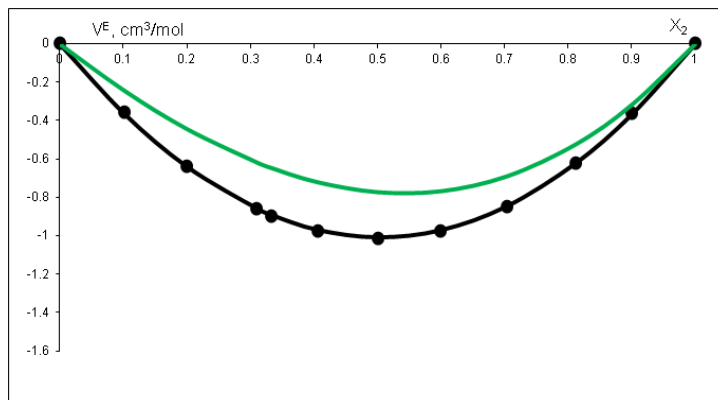


Figure 1. Dependence of excess molar volume on the mole fraction of the organic component. The dots represent experimental data, the black line is an approximation, and the green line is a calculation using independent parameters (see explanation in the text).

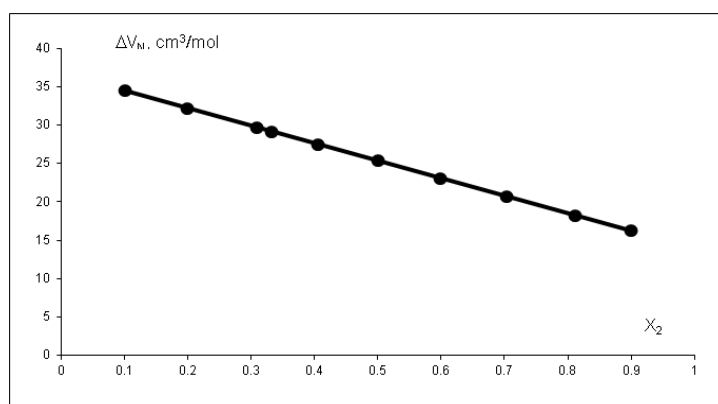


Figure 2. Dependence of function ΔV_N on the mole fraction of the organic component (see text for explanations).

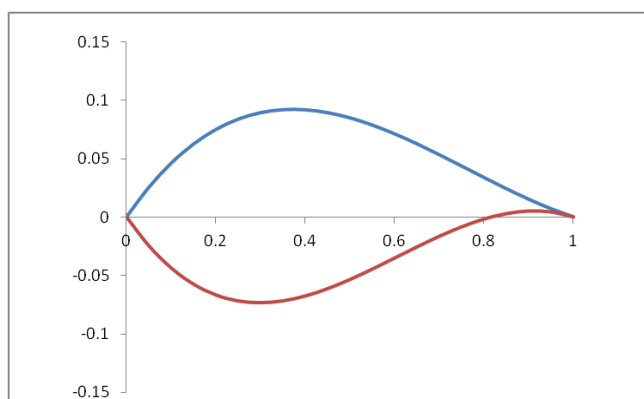


Figure 3. Dependence of functions α^E (blue line) and β^E (red line) on the mole fraction of the organic component (see text for explanations).

Table 1. Structural parameters of the water-organic system (see text for explanations)

	Water	Cosolvent		α^E	β^E
$V_M, \text{cm}^3/\text{mol}$	18.07	40.73	x_{\max}	0.37	0.91
$\bar{V}^\infty, \text{cm}^3/\text{mol}$	14.43	38.17	max	0.092	0.005
$\bar{V}^\circ, \text{cm}^3/\text{mol}$	13.98	36.75	x_{\min}	-	0.30
$\bar{V}^{E^\infty}, \text{cm}^3/\text{mol}$	-3.64	-2.56	min	-	-0.073
$\bar{V}^{E^\circ}, \text{cm}^3/\text{mol}$	-4.09	-3.98	x_0	-	0.82
ξ	0.125	0.553	avg	0.056	-0.036

2. Water-Ethanol

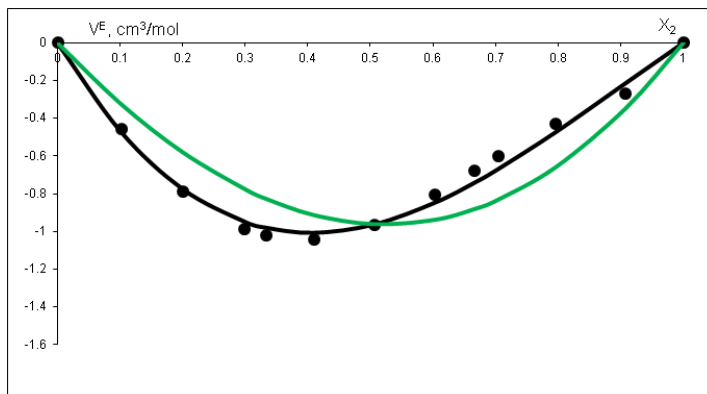


Figure 4. Dependence of excess molar volume on the mole fraction of the organic component. The dots represent experimental data, the black line is an approximation, and the green line is a calculation using independent parameters (see explanation in the text).

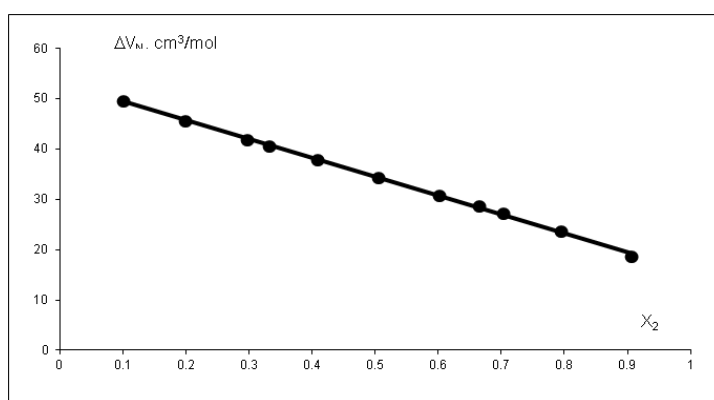


Figure 5. Dependence of function ΔV_N on the mole fraction of the organic component (see text for explanations).

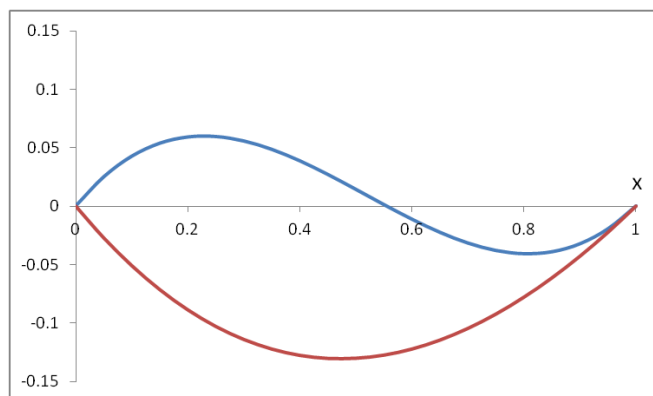


Figure 6. Dependence of functions α^E (blue line) and β^E (red line) on the mole fraction of the organic component (see text for explanations).

Table 2. Structural parameters of the water-organic system (see text for explanations)

	Water	Cosolvent		α^E	β^E
$V_M, \text{cm}^3/\text{mol}$	18.07	58.68	x_{\max}	0.23	-
$\bar{V}^\infty, \text{cm}^3/\text{mol}$	13.86	55.20	max	0.060	-
$\bar{V}^\circ, \text{cm}^3/\text{mol}$	15.81	53.19	x_{\min}	0.81	0.47
$\bar{V}^{E\infty}, \text{cm}^3/\text{mol}$	-4.21	-3.48	min	-0.041	-0.13
$\bar{V}^{E^\circ}, \text{cm}^3/\text{mol}$	-2.26	-5.49	x_0	0.55	-
ξ	-0.464	0.577	avg	0.009	-0.087

3. Water-1-Propanol

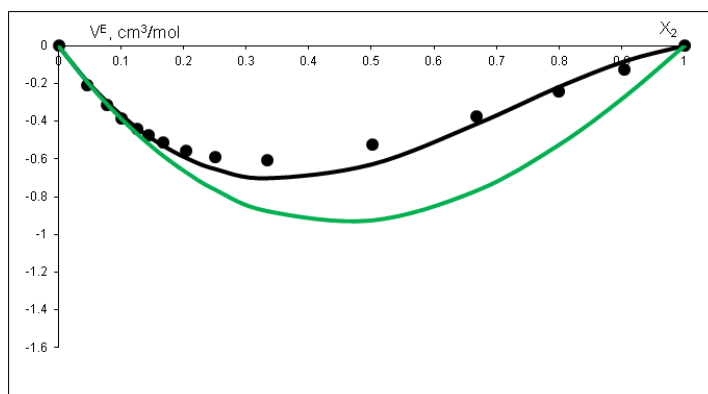


Figure 7. Dependence of excess molar volume on the mole fraction of the organic component. The dots represent experimental data, the black line is an approximation, and the green line is a calculation using independent parameters (see explanation in the text).

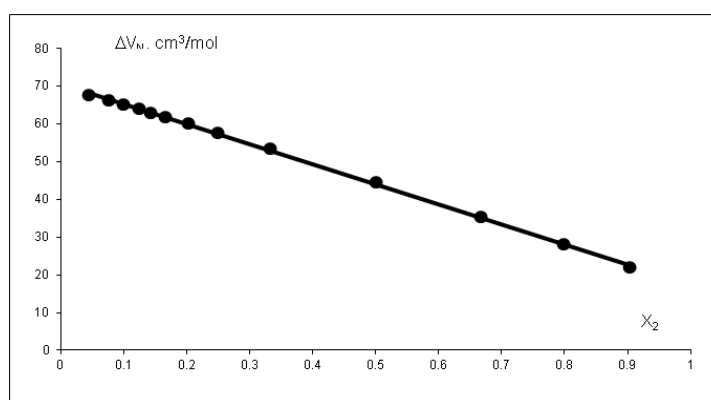


Figure 8. Dependence of function ΔV_N on the mole fraction of the organic component (see text for explanations).

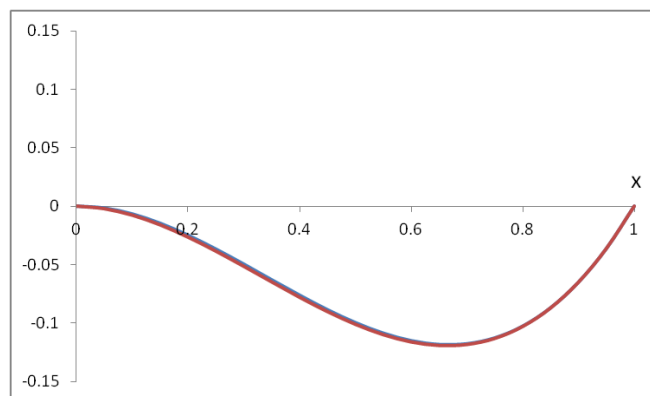


Figure 9. Dependence of functions α^E (blue line) and β^E (red line) on the mole fraction of the organic component (see text for explanations).

Table 3. Structural parameters of the water-organic system (see text for explanations)

	Water	Cosolvent		α^E	β^E
$V_M, \text{cm}^3/\text{mol}$	18.07	75.15	x_{\max}	-	-
$\bar{V}^\infty, \text{cm}^3/\text{mol}$	15.09	70.74	max	-	-
$\bar{V}^\circ, \text{cm}^3/\text{mol}$	17.48	70.71	x_{\min}	0.67	0.67
$\bar{V}^{E^\infty}, \text{cm}^3/\text{mol}$	-2.98	-4.41	min	-0.12	-0.12
$\bar{V}^{E^\circ}, \text{cm}^3/\text{mol}$	-0.59	-4.44	x_0	-	-
ξ	-0.802	0.006	avg	-0.066	-0.067

4. Water-2-Propanol

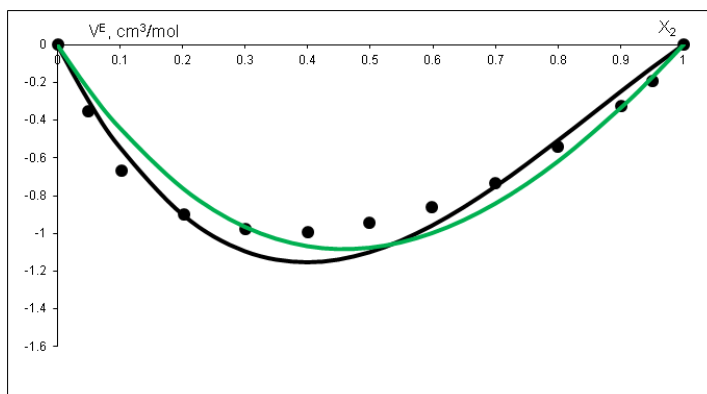


Figure 10. Dependence of excess molar volume on the mole fraction of the organic component. The dots represent experimental data, the black line is an approximation, and the green line is a calculation using independent parameters (see explanation in the text).

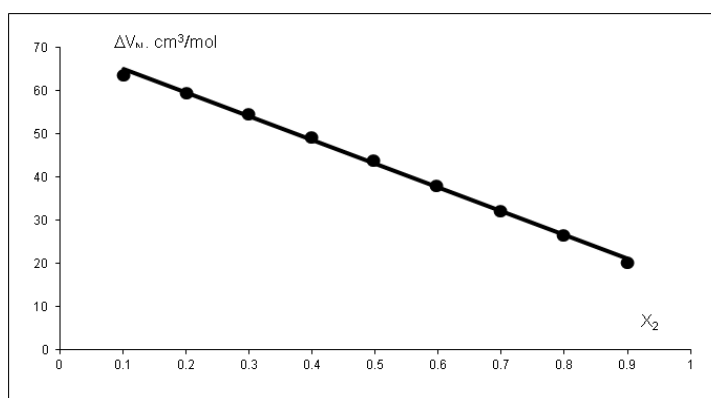


Figure 11. Dependence of function ΔV_N on the mole fraction of the organic component (see text for explanations).

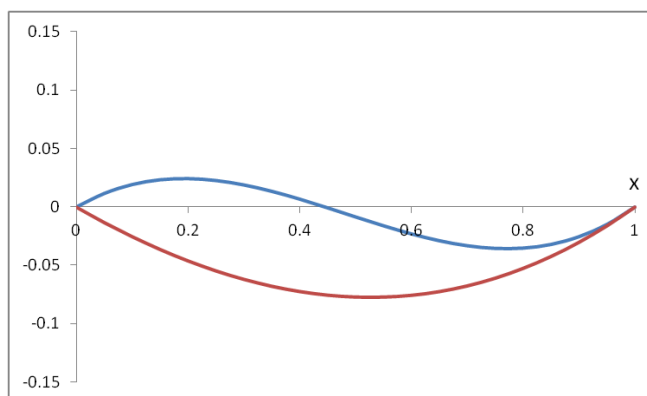


Figure 12. Dependence of functions α^E (blue line) and β^E (red line) on the mole fraction of the organic component (see text for explanations).

Table 4. Structural parameters of the water-organic system (see text for explanations)

	Water	Cosolvent		α^E	β^E
$V_M, \text{cm}^3/\text{mol}$	18.07	76.98	x_{\max}	0.19	-
$\bar{V}^\infty, \text{cm}^3/\text{mol}$	14.51	71.93	max	0.024	-
$\bar{V}^\circ, \text{cm}^3/\text{mol}$	15.73	70.54	x_{\min}	0.77	0.53
$\bar{V}^{E\infty}, \text{cm}^3/\text{mol}$	-3.56	-5.05	min	-0.036	-0.078
$\bar{V}^{E^\circ}, \text{cm}^3/\text{mol}$	-2.34	-6.44	x_0	0.45	-
ξ	-0.343	0.276	avg	-0.006	-0.052

5. Water-Ethylene Glycol

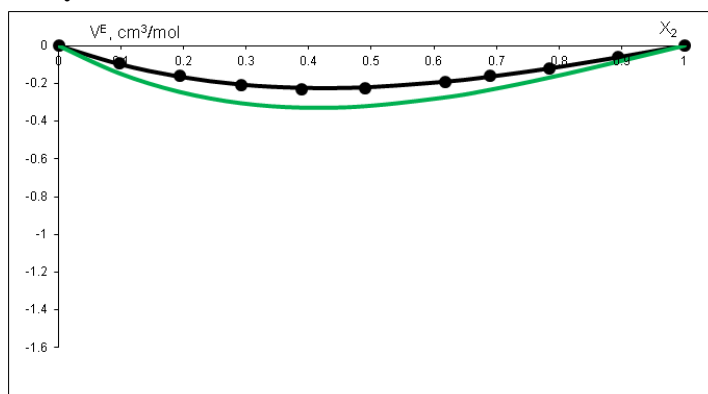


Figure 13. Dependence of excess molar volume on the mole fraction of the organic component. The dots represent experimental data, the black line is an approximation, and the green line is a calculation using independent parameters (see explanation in the text).

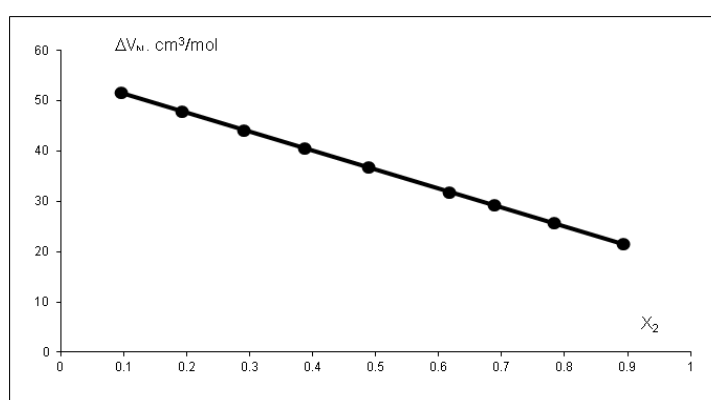


Figure 14. Dependence of function ΔV_N on the mole fraction of the organic component (see text for explanations).

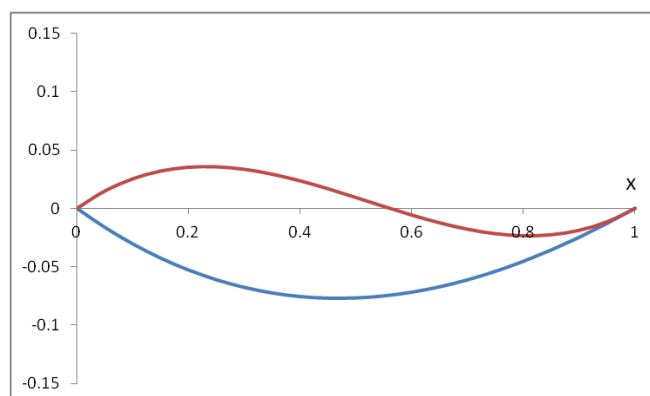


Figure 15. Dependence of functions α^E (blue line) and β^E (red line) on the mole fraction of the organic component (see text for explanations).

Table 5. Structural parameters of the water-organic system (see text for explanations)

	Water	Cosolvent		α^E	β^E
$V_M, \text{cm}^3/\text{mol}$	18.06	56.41	x_{\max}		0.23
$\bar{V}^\infty, \text{cm}^3/\text{mol}$	17.27	54.65	max		0.036
$\bar{V}^\circ, \text{cm}^3/\text{mol}$	17.48	55.26	x_{\min}	0.47	0.81
$\bar{V}^{E\infty}, \text{cm}^3/\text{mol}$	-0.79	-1.76	min	-0.077	-0.023
$\bar{V}^{E^\circ}, \text{cm}^3/\text{mol}$	-0.58	-1.15	x_0		0.56
ξ	-0.268	-0.345	avg	-0.051	0.006

6. Water-Tetrahydrofuran

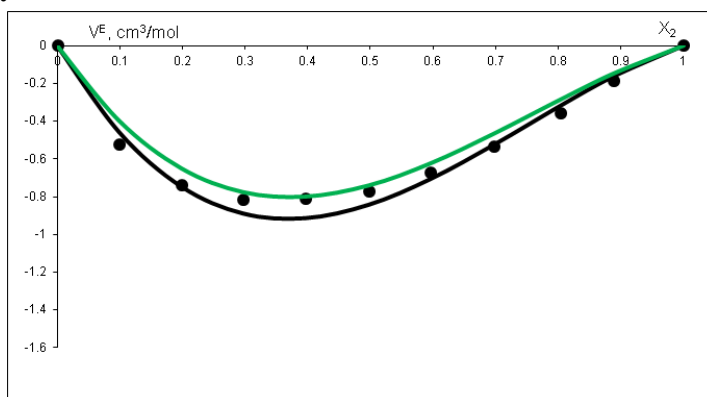


Figure 16. Dependence of excess molar volume on the mole fraction of the organic component. The dots represent experimental data, the black line is an approximation, and the green line is a calculation using independent parameters (see explanation in the text).

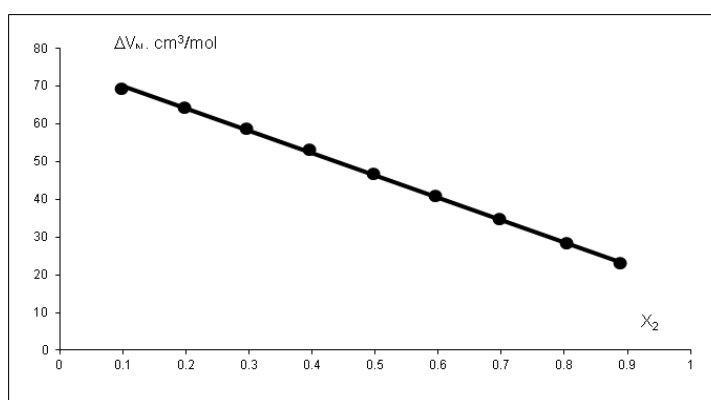


Figure 17. Dependence of function ΔV_N on the mole fraction of the organic component (see text for explanations).

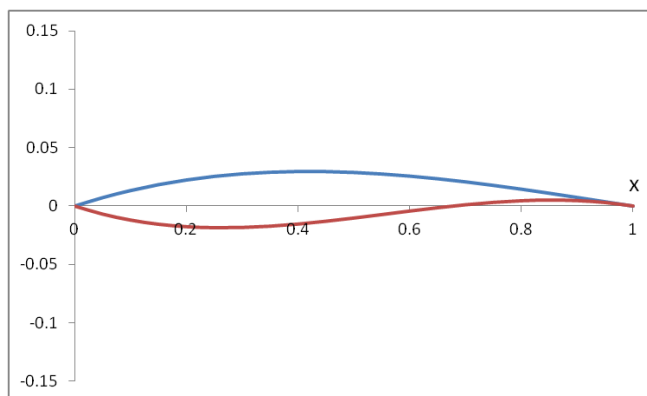


Figure 18. Dependence of functions α^E (blue line) and β^E (red line) on the mole fraction of the organic component (see text for explanations).

Table 6. Structural parameters of the water-organic system (see text for explanations)

	Water	Cosolvent		α^E	β^E
$V_M, \text{cm}^3/\text{mol}$	18.06	81.73	x_{\max}	0.42	0.85
$\bar{V}^\infty, \text{cm}^3/\text{mol}$	17.00	76.90	max	0.030	0.005
$\bar{V}^\circ, \text{cm}^3/\text{mol}$	16.92	76.15	x_{\min}	-	0.26
$\bar{V}^{E\infty}, \text{cm}^3/\text{mol}$	-1.06	-4.83	min	-	-0.019
$\bar{V}^{E^\circ}, \text{cm}^3/\text{mol}$	-1.14	-5.58	x_0	-	0.68
ξ	0.074	0.156	avg	0.019	-0.007

7. Water-1,4-Dioxane

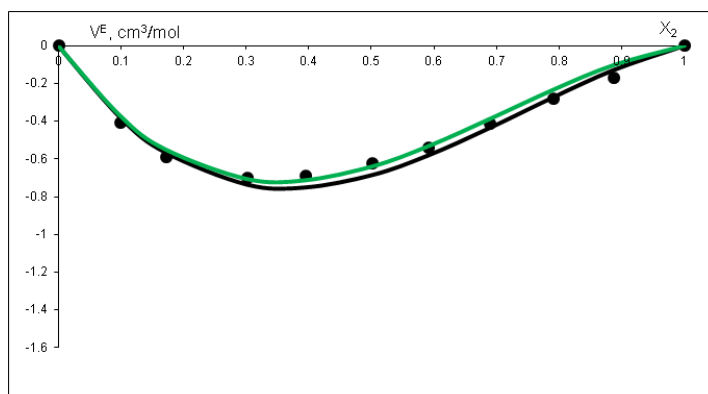


Figure 19. Dependence of excess molar volume on the mole fraction of the organic component. The dots represent experimental data, the black line is an approximation, and the green line is a calculation using independent parameters (see explanation in the text).

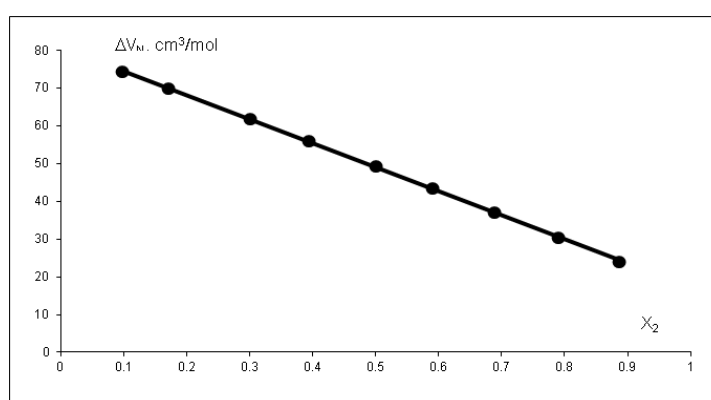


Figure 20. Dependence of function ΔV_N on the mole fraction of the organic component (see text for explanations).

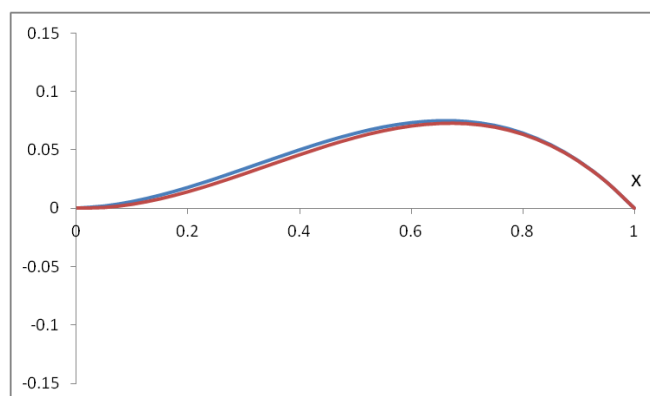


Figure 21. Dependence of functions α^E (blue line) and β^E (red line) on the mole fraction of the organic component (see text for explanations).

Table 7. Structural parameters of the water-organic system (see text for explanations)

	Water	Cosolvent		α^E	β^E
$V_M, \text{cm}^3/\text{mol}$	18.06	85.66	x_{\max}	0.66	0.67
$\bar{V}^\infty, \text{cm}^3/\text{mol}$	17.49	81.10	max	0.075	0.073
$\bar{V}^\circ, \text{cm}^3/\text{mol}$	17.20	81.03	x_{\min}	-	-
$\bar{V}^{E\infty}, \text{cm}^3/\text{mol}$	-0.57	-4.56	min	-	-
$\bar{V}^{E^\circ}, \text{cm}^3/\text{mol}$	-0.86	-4.63	x_0	-	-
ξ	0.498	0.014	avg	0.043	0.040

8. Water-Acetonitrile

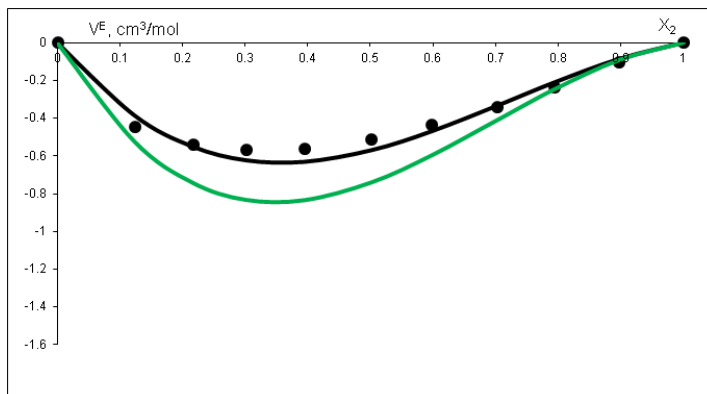


Figure 22. Dependence of excess molar volume on the mole fraction of the organic component. The dots represent experimental data, the black line is an approximation, and the green line is a calculation using independent parameters (see explanation in the text).

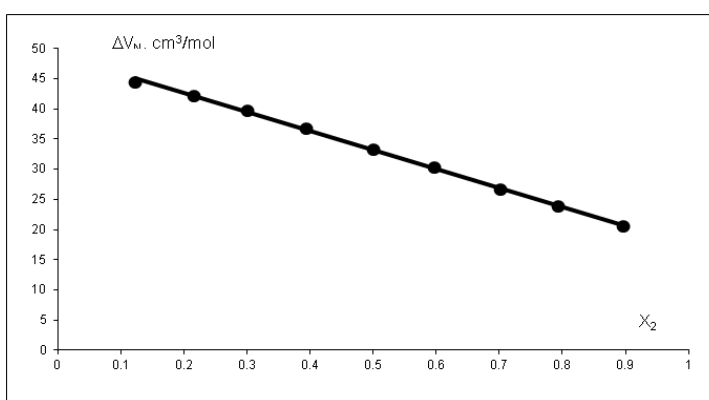


Figure 23. Dependence of function ΔV_N on the mole fraction of the organic component (see text for explanations).

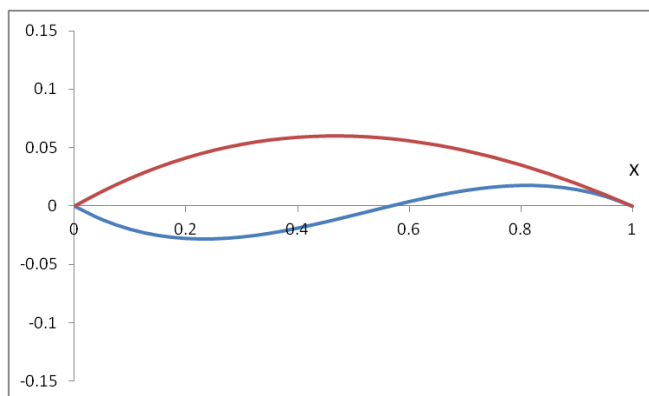


Figure 24. Dependence of functions α^E (blue line) and β^E (red line) on the mole fraction of the organic component (see text for explanations).

Table 8. Structural parameters of the water-organic system (see text for explanations)

	Water	Cosolvent		α^E	β^E
$V_M, \text{cm}^3/\text{mol}$	18.06	52.87	x_{\max}	0.81	0.47
$\bar{V}^\infty, \text{cm}^3/\text{mol}$	17.58	47.42	max	0.018	0.060
$\bar{V}^\circ, \text{cm}^3/\text{mol}$	17.48	48.89	x_{\min}	0.23	-
$\bar{V}^{E^\infty}, \text{cm}^3/\text{mol}$	-0.48	-5.45	min	-0.028	-
$\bar{V}^{E^\circ}, \text{cm}^3/\text{mol}$	-0.58	-3.98	x_0	0.57	-
ξ	0.207	-0.270	avg	-0.005	0.040

9. Water-Acetone

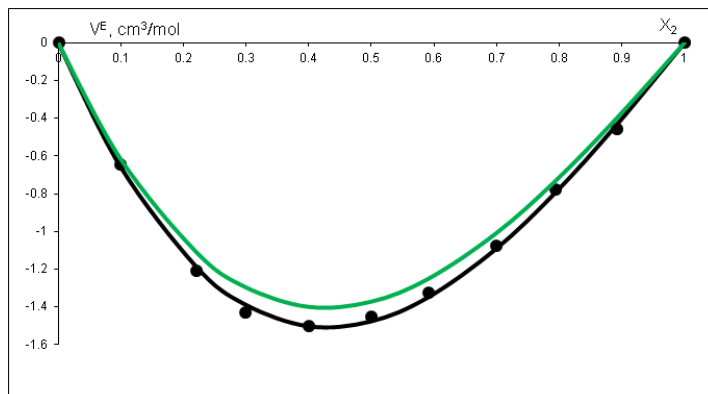


Figure 25. Dependence of excess molar volume on the mole fraction of the organic component. The dots represent experimental data, the black line is an approximation, and the green line is a calculation using independent parameters (see explanation in the text).

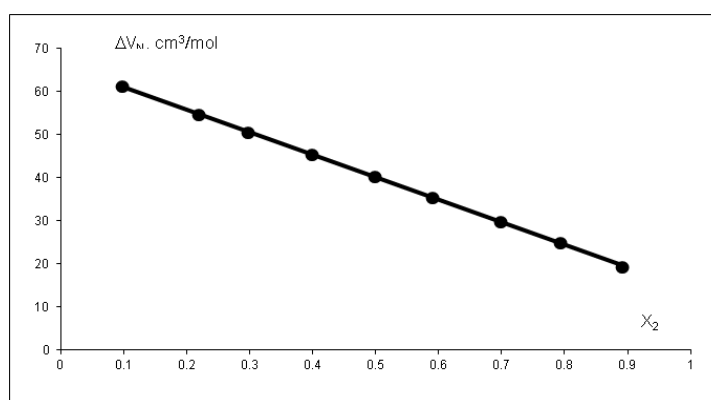


Figure 26. Dependence of function ΔV_N on the mole fraction of the organic component (see text for explanations).

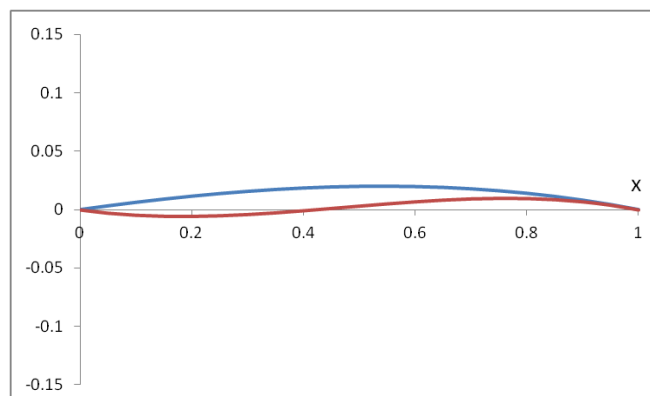


Figure 27. Dependence of functions α^E (blue line) and β^E (red line) on the mole fraction of the organic component (see text for explanations).

Table 9. Structural parameters of the water-organic system (see text for explanations)

	Water	Cosolvent		α^E	β^E
$V_M, \text{cm}^3/\text{mol}$	18.07	74.02	x_{\max}	0.54	0.76
$\bar{V}^\infty, \text{cm}^3/\text{mol}$	14.30	66.80	max	0.020	0.010
$\bar{V}^\circ, \text{cm}^3/\text{mol}$	13.95	66.32	x_{\min}	-	0.18
$\bar{V}^{E\infty}, \text{cm}^3/\text{mol}$	-3.77	-7.22	min	-	-0.006
$\bar{V}^{E^\circ}, \text{cm}^3/\text{mol}$	-4.12	-7.70	x_0	-	0.42
ξ	0.093	0.067	avg	0.013	0.002

10. Water-Dimethylformamide

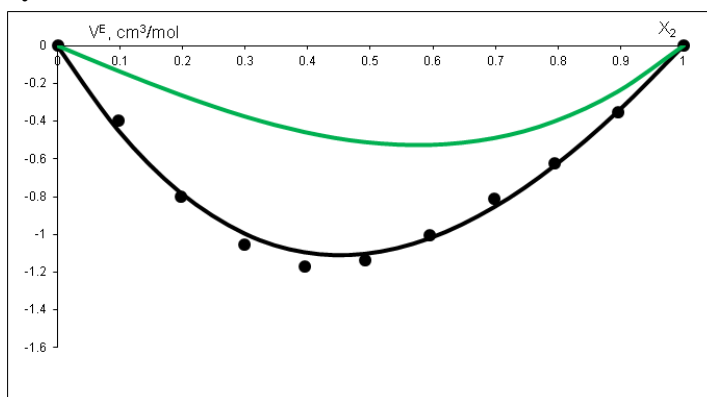


Figure 28. Dependence of excess molar volume on the mole fraction of the organic component. The dots represent experimental data, the black line is an approximation, and the green line is a calculation using independent parameters (see explanation in the text).

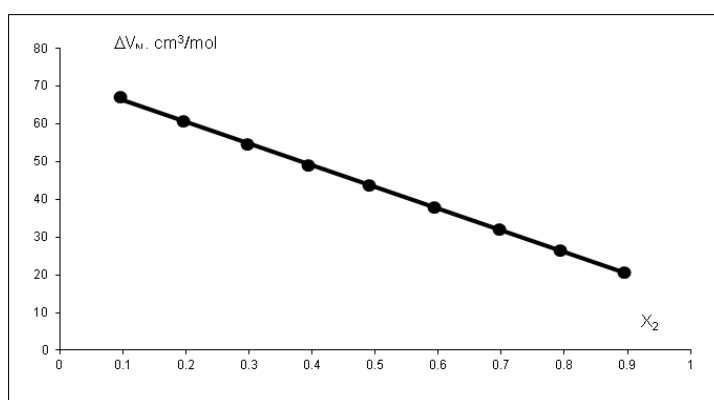


Figure 29. Dependence of function ΔV_N on the mole fraction of the organic component (see text for explanations).

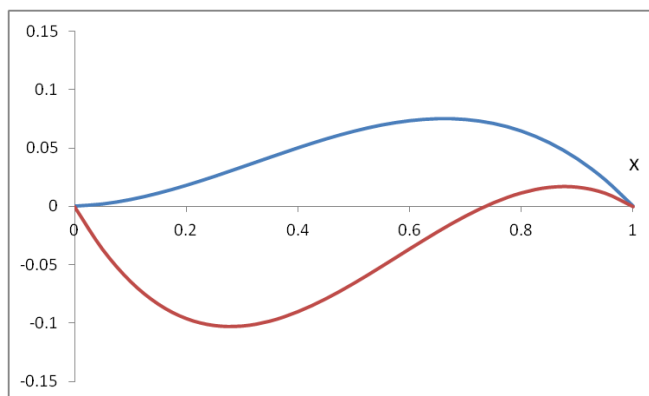


Figure 30. Dependence of functions α^E (blue line) and β^E (red line) on the mole fraction of the organic component (see text for explanations).

Table 10. Structural parameters of the water-organic system (see text for explanations)

	Water	Cosolvent		α^E	β^E
$V_M, \text{cm}^3/\text{mol}$	18.06	77.38	x_{\max}	0.40	0.88
$\bar{V}^\infty, \text{cm}^3/\text{mol}$	15.35	74.50	max	0.147	0.017
$\bar{V}^\circ, \text{cm}^3/\text{mol}$	14.54	72.12	x_{\min}	-	0.28
$\bar{V}^{E\infty}, \text{cm}^3/\text{mol}$	-2.71	-2.88	min	-	-0.103
$\bar{V}^{E^\circ}, \text{cm}^3/\text{mol}$	-3.52	-5.26	x_0	-	0.73
ξ	0.299	0.825	avg	0.093	-0.044

11. Water-Dimethylacetamide

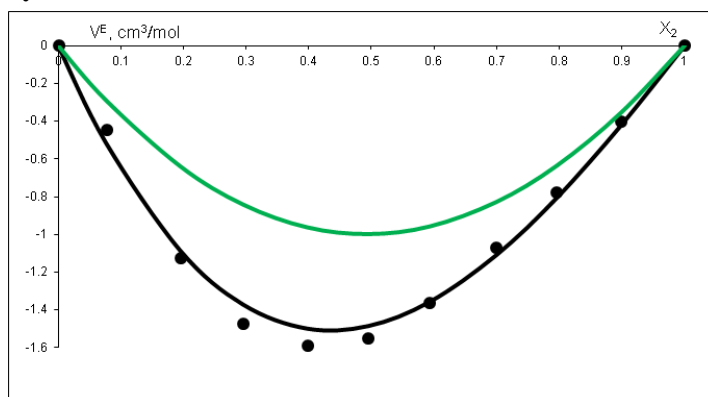


Figure 31. Dependence of excess molar volume on the mole fraction of the organic component. The dots represent experimental data, the black line is an approximation, and the green line is a calculation using independent parameters (see explanation in the text).

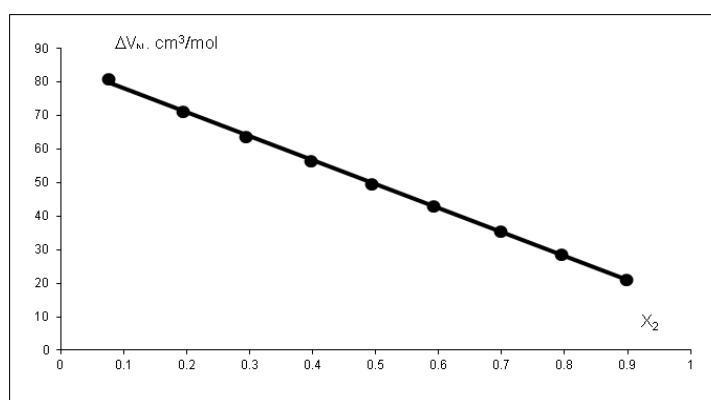


Figure 32. Dependence of function ΔV_N on the mole fraction of the organic component (see text for explanations).

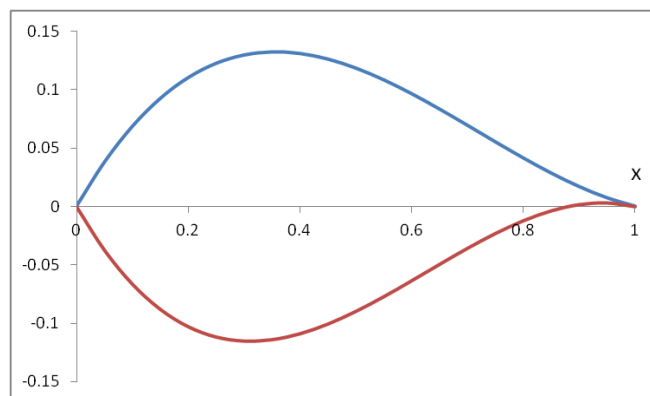


Figure 33. Dependence of functions α^E (blue line) and β^E (red line) on the mole fraction of the organic component (see text for explanations).

Table 11. Structural parameters of the water-organic system (see text for explanations)

	Water	Cosolvent		α^E	β^E
$V_M, \text{cm}^3/\text{mol}$	18.06	93.02	x_{\max}	0.36	0.94
$\bar{V}^\infty, \text{cm}^3/\text{mol}$	14.21	88.90	max	0.132	0.003
$\bar{V}^\circ, \text{cm}^3/\text{mol}$	13.77	85.47	x_{\min}	-	0.31
$\bar{V}^{E\infty}, \text{cm}^3/\text{mol}$	-3.85	-4.12	min	-	-0.115
$\bar{V}^{E^\circ}, \text{cm}^3/\text{mol}$	-4.29	-7.54	x_0	-	0.88
ξ	0.114	0.832	avg	0.079	-0.060

12. Water-Dimethyl Sulfoxide

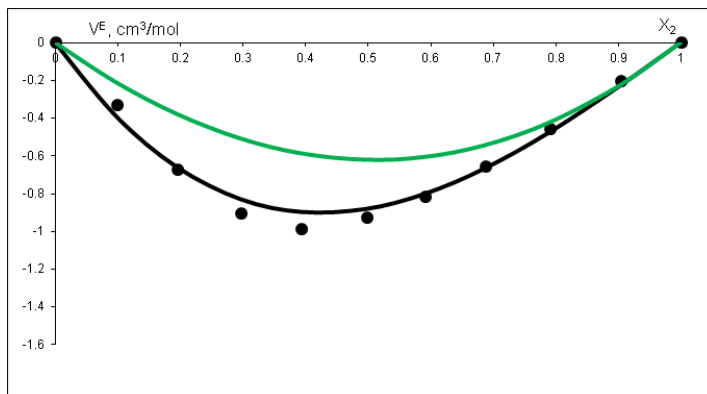


Figure 34. Dependence of excess molar volume on the mole fraction of the organic component. The dots represent experimental data, the black line is an approximation, and the green line is a calculation using independent parameters (see explanation in the text).

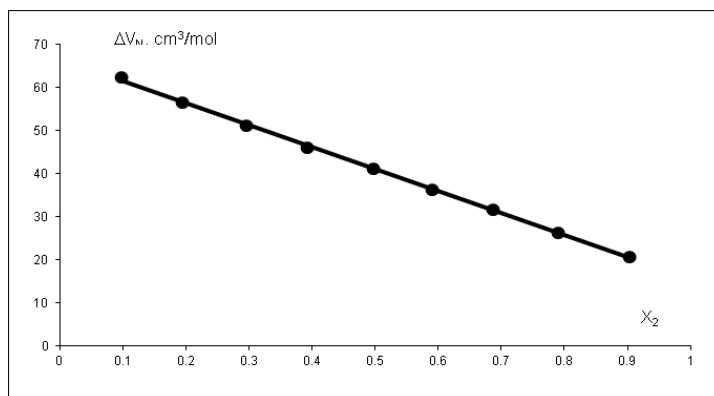


Figure 35. Dependence of function ΔV_M on the mole fraction of the organic component (see text for explanations).

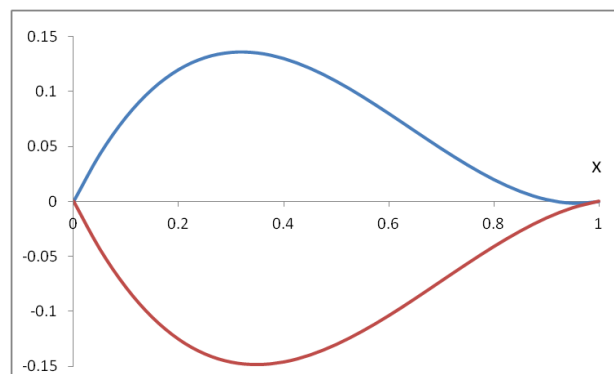


Figure 36. Dependence of functions α^E (blue line) and β^E (red line) on the mole fraction of the organic component (see text for explanations).

Table 12. Structural parameters of the water-organic system (see text for explanations)

	Water	Cosolvent		α^E	β^E
$V_M, \text{cm}^3/\text{mol}$	18.06	71.29	x_{\max}	0.32	-
$\bar{V}^\infty, \text{cm}^3/\text{mol}$	15.46	68.92	max	0.136	-
$\bar{V}^\circ, \text{cm}^3/\text{mol}$	15.67	66.65	x_{\min}	0.96	0.35
$\bar{V}^{E\infty}, \text{cm}^3/\text{mol}$	-2.60	-2.37	min	-0.002	-0.148
$\bar{V}^{E^\circ}, \text{cm}^3/\text{mol}$	-2.39	-4.64	x_0	0.92	-
ξ	-0.082	0.959	avg	0.073	-0.087

Results and discussion

The presented analysis results are determined by only two parameters, ξ_w and ξ_s . Figure 37 shows the relationship between these parameters. It can be seen that no correlation is observed. At the same time, some patterns of distribution can be noted depending on the nature of the organic component.

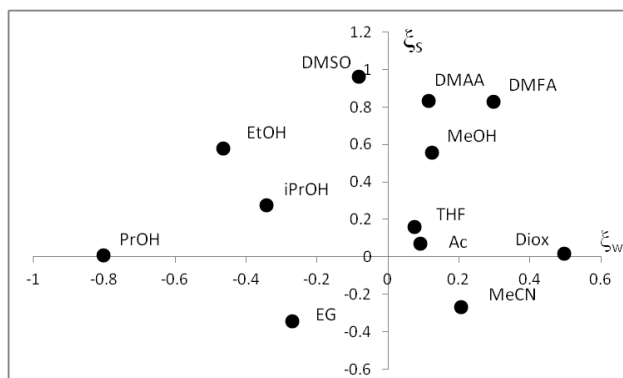


Figure 37. Parameters ξ for aqueous-organic mixtures. The organic component is indicated

For instance, systems with aprotic strongly polar components are grouped in the upper part of the diagram. Protic systems tend toward the left part of the diagram.

Since the systems differ only in their organic component, it is logical to look for a correlation between the calculated parameters and the properties of organic solvents. Indeed, Figure 38 shows that there is a certain correlation between the calculated properties and the polarity of the organic component.

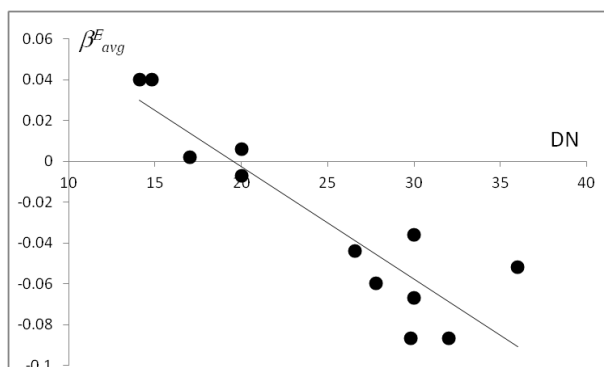


Figure 38. Dependence of the average value of function β^E on the donor number of the organic component

Table 13. Weighting factors of quasi-solvates for equimolar aqueous-organic systems

Cosolvent	w_{11}	w_{22}	w_{12}	w_{21}
Methanol	0.17	0.17	0.28	0.39
Ethanol	0.24	0.24	0.13	0.39
1-Propanol	0.35	0.35	0.05	0.25
2-Propanol	0.26	0.26	0.16	0.32
Ethylene Glycol	0.33	0.33	0.18	0.16
Tetrahydrofuran	0.22	0.22	0.27	0.29
1,4-Dioxane	0.19	0.19	0.37	0.25
Acetonitrile	0.26	0.26	0.30	0.18
Acetone	0.23	0.23	0.27	0.27
DMFA	0.11	0.11	0.32	0.46
DMAA	0.13	0.13	0.28	0.46
DMSO	0.14	0.14	0.23	0.49

In the series of alcohols, there is a clear trend toward a decrease in water-alcohol contacts, as evidenced by the change in the α^E function. This is confirmed by numerous studies [1, 3–5, 15, 17, 23,

25, 26] showing that alcohol systems are characterized by an increasing manifestation of microheterogeneity. This is due to the influence of the hydrophobic part of the molecule and its structure, which leads to differences between propanol and isopropanol, bringing the latter closer to ethanol. It is interesting to note that the compositions at the maxima of the α^E function in systems with methanol and ethanol coincide with the extrema in the mixing heat dependencies of the corresponding systems. Table 13 presents the calculated weighting functions Eq. 10–13 for an equimolar mixture. In the case of a stochastic system, they are all equal to 0.25. The sum of w_{12} and w_{21} can be used as a rough estimate of miscibility.

Figure 39 shows the dependence of the sum of weighting factors for alcohols on the number of carbon atoms. Extrapolation to butanol indicates a near-total absence of mixing. The position of the minimum of the β^E function is noteworthy. For instance, in the system with methanol, it corresponds to an alcohol-to-water ratio of 1:2; for ethanol and isopropanol, it is 1:1; and for propanol, it is 2:1.

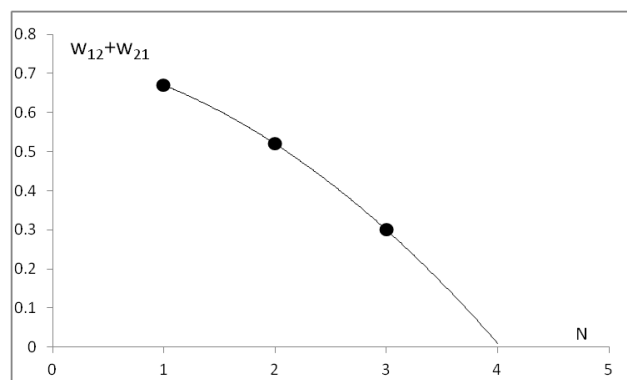


Figure 39. Dependence of the sum of weighting factors on the number of carbon atoms for equimolar aqueous-alcohol mixtures.

The structure of the water–ethylene glycol mixture fundamentally differs from systems with monohydric alcohols. Ethylene glycol stands out among all considered systems due to the negative values of parameters ξ_w and ξ_s . The behavior of the β^E function indicates that role asymmetry is suppressed in the system, which may imply the formation of local structures with a spatial network of hydrogen bonds; this is generally consistent with literature data [18]. Due to the presence of two OH-groups at the ends of the molecule, ethylene glycol does not disrupt the water structure but rather integrates into it, acting as a bridge. Each ethylene glycol molecule can form up to 6 hydrogen bonds (as both a donor and an acceptor). Instead of micro-separation (as seen, for example, in propanol systems), a single hybrid framework is formed here, where water and glycol molecules are completely mixed at the molecular level. The mixture behaves almost like an ideal solution in terms of particle distribution.

Tetrahydrofuran and water show a negligible deviation from the base model. This does not imply an absence of structure, as role asymmetry is already inherent in the model itself. As studies show [8, 28], THF has the ideal molecular size to fit into the cavities of the water framework. Water molecules tend to surround the THF ring, creating quasi-clathrate structures. At a THF mole fraction of about 0.19, the structure reaches its maximum ordering. At intermediate concentrations, modeling detects tortuous channels of THF molecules interwoven with similar channels of water molecules.

For the system with dioxane, positive values of the α^E and β^E functions are observed, with a maximum corresponding to a dioxane-to-water ratio of 2:1, suggesting an enhancement of dioxane's role as a solvent. The structure of the water–1,4-dioxane mixture is notable because dioxane has two symmetrically located oxygen atoms and lacks an intrinsic dipole moment in its "chair" conformation. This creates a unique type of interaction with water. The dioxane molecule often acts as a bridge, linking two different water clusters. Table 13 shows that for an equimolar dioxane-water mixture, quasi-solvates of the Q_{ws} type predominate. At the same time, modern MD simulations show [19, 27] that at equimolar compositions, the system represents two interwoven labyrinths. One labyrinth consists of water molecules linked into infinite chains, while the other consists of dioxane molecules touching each other with their hydrophobic faces. These labyrinths hardly mix at the atomic level, making contact only at the points of hydrogen bonding.

Acetonitrile – Water. This system differs sharply from others in terms of the topology of α^E and β^E functions. The role of acetonitrile as a solvent is enhanced. The α^E function changes its sign. As research shows [6, 7, 9], the structure of the water–acetonitrile mixture is anomalous among all solvents miscible with water. The system is characterized by a very weak bond between the components and a strong tendency toward microphase separation. Acetonitrile is a very poor partner for hydrogen bonding. Its -CN group interacts with water much more weakly than water–water bonds.

The parameters of the water–acetone system practically do not differ from the base model and, in terms of topology, coincide with the THF system. Acetone is notable for its combination of the strong polarity of the carbonyl group and the hydrophobicity of its two methyl groups. This creates a micro-heterogeneous system that balances between complete mixing and nanophase separation. Acetone does not form chains (like alcohols) but tends to group into bulky aggregates. The methyl groups of acetone orient toward each other, forming hydrophobic cores. Water surrounds these cores, creating a complex topology that modern MD models describe as a "loose sponge"[22].

The systems with DMF, DMAA, and DMSO share a similar topology of the α^E and β^E functions. The cosolvent molecules act as super-acceptors of hydrogen bonds and attract water molecules significantly more strongly than water molecules attract each other. Terahertz spectroscopy and other studies [8, 20, 22, 29] confirm that the most stable structural unit is a complex consisting of one cosolvent molecule and two water molecules. This explains the peak in heat evolution at a mole fraction of 0.33. At this point, practically all free water disappears, transforming into the hydration shell of the organic solvent. In this regard, it is worth noting the presence of a minimum of β^E precisely at this component ratio.

Thus, having analyzed 12 aqueous-organic systems using the extended BAQS model, it can be concluded that, despite the apparent simplicity of the model, this approach allows for the detection of qualitative and, in some cases, quantitative patterns in the structural characteristics of non-electrolyte solutions.

Conclusions

An extended model of binary additive quasi-solvates (BAQS) is proposed to describe the properties of mixed solvents. The model incorporates a priori information regarding the limiting partial molar properties of the components, using these to calculate corresponding effective properties. The discrepancy between the effective and a priori values is interpreted as a change in the weighting factors of the quasi-solvates. Structural changes are described by two functions: excess heterogeneity, α^E and excess role asymmetry, β^E .

Using molar volume data for 12 aqueous–organic systems, structural parameters were calculated within the extended BAQS model. While the specific nature of the model precludes a direct comparison with established thermodynamic and structural quantities, the identified patterns in the distribution of structural parameters generally correlate with experimental data and molecular modeling results.

The inherent simplicity of the proposed approach makes it suitable for the rapid analysis of large datasets of liquid systems.

Acknowledgements

The authors acknowledge the Ministry of Education and Science of Ukraine for the Grant No. 0126U003820 under the program KPK 2201390.

Conflict of Interest: The authors declare no conflict of interest.

Authors Contributions: All authors have contributed equally to this work.

References

1. Ågren, H., et al., Ethanol in Aqueous Solution Studied by Microjet Photoelectron Spectroscopy and Theory. *Accounts of Chemical Research*, 2022. **55**(21): p. 3080–3087. <https://doi.org/10.1021/acs.accounts.2c00471>
2. Aminabhavi, T. M., Gopalakrishna, B. Density, Viscosity, Refractive Index, and Speed of Sound in Aqueous Mixtures of N,N-Dimethylformamide, Dimethyl Sulfoxide, N,N-Dimethylacetamide,

- Acetonitrile, Ethylene Glycol, Diethylene Glycol, 1,4-Dioxane, Tetrahydrofuran, 2-Methoxyethanol, and 2-Ethoxyethanol at 298.15 K. *J. Chem. Eng. Data*, 1995. **40**(4): p. 856–861. <https://doi.org/10.1021/je00020a026>
3. Atamas, N., et al., Clustering in Water-Propanol Solutions. *2021 IEEE 11th International Conference Nanomaterials: Applications & Properties (NAP)*, 2021. p. 1–5. <https://doi.org/10.1109/NAP51885.2021.9568589>
 4. Bai, H.-J., et al., Insights into Ethanol–Water Clusters in Alcoholic Beverages by Vibration Spectroscopy Connecting with Quality and Taste. *J. Mol. Liq.*, 2023. **390**: p. 123057. <https://doi.org/10.1016/j.molliq.2023.123057>
 5. Böhm, J., et al., Water-Methanol Mixtures: Investigations of Their Peculiar Mixing Properties by Means of Molecular Dynamics Simulations. *J. Mol. Liq.*, 2025. **425**: p. 127194. <https://doi.org/10.1016/j.molliq.2025.127194>
 6. Bouazizi, S., et al., Structural and dynamical properties of water–acetonitrile mixture studied by molecular dynamics and enhanced via machine learning. *The European Physical Journal Special Topics*, 2026. <https://doi.org/10.1140/epjs/s11734-026-02219-9>
 7. Bouazizi, S., et al., Structural and Dynamical Insights into Acetonitrile-Water Mixtures: A Molecular Dynamics Study of Self-Diffusion, Reorientational Correlation Times, and Temperature-Dependent Behavior. *ACS Omega*, 2025. **10**(33): p. 38092–38102. <https://doi.org/10.1021/acsomega.5c05444>
 8. Bozorova, D., et al., Heteromolecular Structure Formation in Binary Solutions of Dimethylformamide-Water and Tetrahydrofuran-Water: Ftir and Refractometry. *Latv. J. Phys. Tech. Sci.*, 2025. **62**(4): p. 14–28. <https://doi.org/10.2478/lpts-2025-0026>
 9. Chen, J., Sit, P. H.-L. Ab Initio Study of the Structural Properties of Acetonitrile–Water Mixtures. *Chem. Phys.*, 2015. **457**: p. 87–97. <https://doi.org/10.1016/j.chemphys.2015.05.022>
 10. De Visser, C., et al., Thermodynamic Properties of Binary Mixtures. Part 1.—Isobaric Excess Heat Capacities and Excess Molar Volumes of Dimethyl Sulphoxide + Water Mixtures at 298.15 K. *J. Chem. Soc., Faraday Trans. 1*, 1978. **74**: p. 1159–1169. <https://doi.org/10.1039/F19787401159>
 11. Easteal, A. J., Woolf, L. A. (p, Vm, T, x) Measurements for $\{(1 - x)\text{H}_2\text{O} + x\text{CH}_3\text{CN}\}$ in the Range 278 to 323 K and 0.1 to 280 MPa I. Experimental Results, Isothermal Compressibilities, Isobaric Expansivities, and Partial Molar Volumes. *J. Chem. Thermodyn.*, 1988. **20**(6): p. 693–699. [https://doi.org/10.1016/0021-9614\(88\)90020-1](https://doi.org/10.1016/0021-9614(88)90020-1)
 12. Efimov, P., Analysis of volumetric properties of liquid mixtures: I. Method of binary additive quasi-solvates. *V. N. Karazin Kharkiv National University Bulletin. Chemical Series*, 2023. **(41)**: p. 32–41. <https://doi.org/10.26565/2220-637X-2023-41-03>
 13. Estrada-Baltazar, A., et al., Experimental Densities and Excess Volumes for Binary Mixtures Containing Propionic Acid, Acetone, and Water from 283.15 K to 323.15 K at Atmospheric Pressure. *J. Chem. Eng. Data*, 2003. **48**(6): p. 1425–1431. <https://doi.org/10.1021/je030102f>
 14. González, B., et al., Density and Viscosity Experimental Data of the Ternary Mixtures 1-Propanol or 2-Propanol + Water + 1-Ethyl-3-methylimidazolium Ethylsulfate. Correlation and Prediction of Physical Properties of the Ternary Systems. *J. Chem. Eng. Data*, 2008. **53**(3): p. 881–887. <https://doi.org/10.1021/je700700f>
 15. Guo, S., et al., A Theoretical Study on Intermolecular Hydrogen Bonds of Isopropanol-Water Clusters. *Theor. Chem. Acc.*, 2022. **141**: p. 6. <https://doi.org/10.1007/s00214-022-02865-x>
 16. Herráez, J. V., Belda, R. Refractive Indices, Densities and Excess Molar Volumes of Monoalcohols + Water. *J. Solution Chem.*, 2006. **35**(9): p. 1315–1328. <https://doi.org/10.1007/s10953-006-9059-4>
 17. Hu, X., et al., Investigation of Liquor Microstructure (Ethanol-Water Clusters): Molecular Dynamics Simulation and Density Functional Theory. *J. Mol. Graph. Model.*, 2024. **133**: p. 108864. <https://doi.org/10.1016/j.jmglm.2024.108864>
 18. Huot, J. Y., et al., A Comprehensive Thermodynamic Investigation of Water-Ethylene Glycol Mixtures at 5, 25, and 45 °C. *J. Solution Chem.*, 1988. **17**(7): p. 601–636. <https://doi.org/10.1007/BF00645974>

19. Kolaříková, A., et al., Concentration Fluctuation/Microheterogeneity Duality Illustrated with Aqueous 1,4-Dioxane Mixtures. *J. Chem. Theory Comput.*, 2024. **20**(9): p. 3473–3483. <https://doi.org/10.1021/acs.jctc.4c00151>
20. Koverga, V., et al., Local Structure of DMF–Water Mixtures, as Seen from Computer Simulations and Voronoi Analysis. *J. Phys. Chem. B*, 2022. **126**(36): p. 7013–7024. <https://doi.org/10.1021/acs.jpcc.2c02235>
21. Lepori, L., Gianni, P. Partial Molar Volumes of Ionic and Nonionic Organic Solutes in Water: A Simple Additivity Scheme Based on the Intrinsic Volume Approach. *J. Solution Chem.*, 2000. **29**(5): p. 405–447. <https://doi.org/10.1023/A:1005150616038>
22. Lotze, S., et al., Femtosecond Mid-Infrared Study of the Dynamics of Water Molecules in Water-Acetone and Water-Dimethyl Sulfoxide Mixtures. *J. Phys. Chem. B*, 2015. **119**(16): p. 5228–5239. <https://doi.org/10.1021/jp512703w>
23. Lü, L., et al., Roles of Hydrogen Bonding Interactions and Hydrophobic Effects on Enhanced Water Structure Strength in Aqueous Alcohol Solutions. *Physics of Fluids*, 2023. **35**(3): p. 032014. <https://doi.org/10.1063/5.0142699>
24. Marsh, K. N., Richards, A. E. Excess Volumes for Ethanol + Water Mixtures at 10 K Intervals from 278.15 to 338.15 K. *Aust. J. Chem.*, 1980. **33**(10): p. 2121–2132. <https://doi.org/10.1071/CH9802121>
25. Morbidini, R., et al., Molecular structural dynamics in water–ethanol mixtures: Spectroscopy with polarized neutrons simultaneously accessing collective and self-diffusion. *The Journal of Chemical Physics*, 2023. **159**(22): p. 221103. <https://doi.org/10.1063/5.0174448>
26. Moschos, V., et al., Dynamically and structurally heterogeneous 1-propanol/water mixtures. *The Journal of Chemical Physics*, 2023. **159**(16): p. 164903. <https://doi.org/10.1063/5.0170504>
27. Nagy, P. I., et al., Monte Carlo structure simulations for aqueous 1,4-dioxane solutions. *The Journal of Physical Chemistry B*, 2008. **112**(7): p. 2085–2094. <https://doi.org/10.1021/jp075603c>
28. Noguchi, N., et al., Similarities between the tetrahydrofuran clathrate hydrate after pressure-induced amorphization and aqueous tetrahydrofuran solution: an in situ Raman and infrared spectroscopic study. *Physical Chemistry Chemical Physics*, 2025. **27**(23): p. 12427–12437. <https://doi.org/10.1039/d5cp01016k>
29. Pathania, A., et al., Slowdown of Solvent Structural Dynamics in Aqueous DMF Solutions. *Chem. Phys. Impact*, 2024. **9**: p. 100711. <https://doi.org/10.1016/j.chphi.2024.100711>
30. Pruett, D. J., Felker, L. K. Densities and Apparent Molar Volumes in the Binary System Dimethyl Sulfoxide–Water at 25, 40, 60, and 65 °C. *J. Chem. Eng. Data*, 1985. **30**(4): p. 452–455. <https://doi.org/10.1021/je00042a025>
31. Raj, A., et al., Raman Spectra and Structure of Hydrogen-Bonded Water Oligomers in Tetrahydrofuran–H₂O Binary Solutions. *J. Raman Spectrosc.*, 2022. **53**(10): p. 1710–1721. <https://doi.org/10.1002/jrs.6381>
32. Sakurai, M. Partial Molar Volumes for 1,4-Dioxane + Water. *J. Chem. Eng. Data*, 1992. **37**(4): p. 492–496. <https://doi.org/10.1021/je00008a027>
33. Sakurai, M. Partial Molar Volumes for Acetonitrile + Water. *J. Chem. Eng. Data*, 1992. **37**(3): p. 358–362. <https://doi.org/10.1021/je00007a023>
34. Sakurai, M. Partial Molar Volumes of Ethylene Glycol and Water in Their Mixtures. *J. Chem. Eng. Data*, 1991. **36**(4): p. 424–427. <https://doi.org/10.1021/je00004a023>
35. Sakurai, M., Nakagawa, T. Apparent Molar Volumes of Water in Methanol and Tetrahydrofuran at 298.15 K. *Bull. Chem. Soc. Jpn.*, 1982. **55**(5): p. 1641–1642. <https://doi.org/10.1246/bcsj.55.1641>
36. Sakurai, M., Nakagawa, T. Densities of Dilute Solutions of Water in Benzene and in Methanol at 278.15, 288.15, 298.15, 308.15, and 318.15 K. Partial Molar Volumes V_w and Values of $\partial V_w / \partial T$ for Water in Benzene and in Methanol. *J. Chem. Thermodyn.*, 1982. **14**(3): p. 269–274. [https://doi.org/10.1016/0021-9614\(82\)90017-9](https://doi.org/10.1016/0021-9614(82)90017-9)
37. Sakurai, M., et al., Densities of Dilute Solutions of Water in n-Alkanols at 278.15, 288.15, 298.15, 308.15, and 318.15 K: Partial Molar Volumes of Water in n-Alkanols. *J. Chem. Thermodyn.*, 1984. **16**(1): p. 71–74. [https://doi.org/10.1016/0021-9614\(84\)90151-4](https://doi.org/10.1016/0021-9614(84)90151-4)
38. Seo, S., et al., Kirkwood-Buff Analysis of Binary and Ternary Systems Consisting of Alcohols (Methanol, Ethanol, 1-Propanol, and 2-Propanol), Water, and n-Hexane to Understand the

- Formation of Surfactant-Free Microemulsions. *The Journal of Physical Chemistry B*, 2024. **128**(20): p. 5092–5108. <https://doi.org/10.1021/acs.jpcc.4c01563>
39. Singh, R., et al., Water structure and dynamics under distinct microheterogeneity in DMSO–water and acetone–water mixtures. *The Journal of Chemical Physics*, 2026. **164**(9): p. 094113. <https://doi.org/10.1063/5.0317907>
40. Trabelsi, S., et al., Intermolecular Interactions in an Equimolar Methanol-Water Mixture: Neutron Scattering, DFT, NBO, AIM, and MD Investigations. *J. Mol. Liq.*, 2022. **349**: p. 118131. <https://doi.org/10.1016/j.molliq.2021.118131>
41. van Meurs, N., Somsen, G. Excess and Apparent Molar Volumes of Mixtures of Water and Acetonitrile Between 0 and 25 °C. *J. Solution Chem.*, 1993. **22**(5): p. 427–436. <https://doi.org/10.1007/BF00647680>
42. Wang, Y., et al., Study of Hydrogen Bonding Interactions in Ethylene Glycol-Water Binary Solutions by Raman Spectroscopy. *Spectrochim. Acta, Part A*, 2021. **260**: p. 119916. <https://doi.org/10.1016/j.saa.2021.119916>
43. Wong, D. B., et al., Water Dynamics in Water/DMSO Binary Mixtures. *J. Phys. Chem. B*, 2012. **116**(18): p. 5479–5490. <https://doi.org/10.1021/jp301967e>

Received 12.03.2026

Revised version 17.04.2026

Accepted 15.05.2026

Published 29.05.2026

П. В. Єфімов, Н. В. Єфімова. Аналіз волюмометричних властивостей рідких сумішей. II. Водно-органічні системи розчинників

Харківський національний університет імені В. Н. Каразіна, навчально-науковий інститут хімії, пл. Свободи 4, 61022, Харків, Україна

Запропоновано розширену модель бінарних адитивних квазісольватів (BAQS) для опису властивостей подвійних рідких систем. Модель містить два додаткові параметри: граничні парціальні молярні величини компонентів розчину. Варто зазначити, що ці параметри визначаються априорі, зазвичай на основі незалежних експериментальних даних. Водночас, у межах моделі, ефективні граничні парціальні молярні величини розраховуються на основі залежності досліджуваної властивості від складу суміші. Розбіжність між априорними та ефективними значеннями пояснюється зсувом рівноваги між гомогенними та гетерогенними квазісольватами, а також перерозподілом ролей «розчинник-розчинена речовина» всередині гетерогенних квазісольватів. Для кожного компонента введено параметр ξ , що є відношенням ефективної надлишкової граничної парціальної молярної величини до її відповідного априорного значення. На основі цих параметрів визначено надлишкові функції гетерогенності α^E та асиметрії ролей β^E .

Використовуючи залежності молярного об'єму від складу для 12 подвійних водних систем (з метанолом, етанолом, 1-пропанолом, 2-пропанолом, етиленгліколем, тетрагідрофураном, 1,4-діоксаном, ацетонітрилом, ацетоном, диметилформамідом, диметилацетамідом та диметилсульфоксидом) при 298.15 K, а також літературні дані, було розраховано функції α^E та β^E . У дослідженні визначено склади та значення функцій в точках екстремумів, середні значення функцій та вагові коефіцієнти квазісольватів для екімолярних сумішей. Результати демонструють, що розраховані параметри можуть ефективно характеризувати структурні особливості водно-органічних розчинів. Попри очевидну простоту моделі, цей підхід є придатним для експрес-аналізу великих масивів даних подвійних рідких систем.

Ключові слова: фізико-хімічний аналіз, молярний об'єм, граничний парціальний молярний об'єм, водно-органічний розчинник, бінарні адитивні квазісольвати.

Конфлікт інтересів: Автори повідомляють про відсутність конфлікту інтересів.

Внесок авторів: Всі автори зробили рівний внесок у цю роботу.

Надіслано до редакції 12.03.2026

Надіслано кінцеву версію 17.04.2026

Прийнято до публікації 15.05.2026

Опубліковано 29.05.2026

Kharkiv University Bulletin. Chemical Series. Issue 46 (69), 2026